Clinical Application of $B3$ Three-Valued Logic and Hyper G-Matrix Theory to Hepatocellular Carcinoma Screening

HASAN KELEŞ[1], UMIT YAVUZ KELEŞ[2]
[1]Department of Mathematics
Karadeniz Technical University
Campus of Kanuni, Ortahisar, 61080 Trabzon
TURKIYE

[2]Department of Gastroenterology
Karadeniz Technical University
Campus of Kanuni, Ortahisar, 61080 Trabzon
TURKIYE

Abstract: This paper presents a groundbreaking mathematical framework that establishes a rigorous connection between two seemingly distinct domains: Keleş's B_3 three-valued logic $\mathcal{B}_3 = \{-1, 0, 1\}$ for clinical decision-making and the theory of Hyper G-matrix pairs $A^{-T} = D_1 B D_2$. We introduce the novel concept of B_3-Hyper G-matrix pairs, denoted $A \bowtie_{\mathcal{B}_3} B$, which unifies these frameworks through a threshold-based encoding function $\phi : \mathbb{R} \to \mathcal{B}_3$. We prove fundamental invariants including sign invariance, risk conservation, and uncertainty propagation. The theoretical results are validated through application to hepatocellular carcinoma (HCC) screening, where the Logical Risk Index (LRI) is shown to be proportional to the trace of a B_3-Hyper G-matrix transformation. This work provides a rigorous mathematical foundation for personalized, evidence-based decision algorithms in clinical medicine.

Key-Words: Hepatocellular Carcinoma, Three-Valued Logic, B3 Framework, Decision Support System, Personalized Medicine, Mathematical Modeling, Hyper G-Matrix, Clinical Decision-Making, Risk Stratification, Monte Carlo Simulation.

Mathematics Subject Classification: 03B50, 62P10, 68T05, 92C50, 92B20, 60J20, 62H30, 90C90, 65C05, 03B48.

PubMed/MeSH Terms: D006528, D008103, D019636, D001185, D057285, D054523, D008439, D008126, D008451, D019046, D018570, D015415, D000511, D008136, D006509, D006526.

ICD-10 Codes: C22.0, K74.6, Z12.89, Z86.19.

LOINC Codes: 20427-7, 1975-2, 1751-7, 19774-2, 11557-6.

SNOMED CT Codes: 363346000, 19943007, 399232008, 71388002, 363787002.

Received: December 14, 2025. Revised: March 27, 2026. Accepted: May 11, 2026. Published: June 24, 2026.

1 Introduction

The management of clinical uncertainty remains a fundamental challenge in medical decision-making. Traditional binary logic systems cannot adequately represent the gray zones inherent in clinical practice—borderline laboratory values, rare etiologies, and missing data. The B_3 three-valued logic framework $\mathcal{B}_3 = \{-1, 0, 1\}$ addresses this limitation, where $+1$ represents definite positive, 0 represents uncertain/indeterminate, and -1 represents definite negative, [1].

Independently, the theory of Hyper G-matrices provides an algebraic framework for relating pairs of matrices through diagonal scaling transformations, [2]. A pair (A, B) is called a Hyper G-matrix pair, denoted $A \bowtie B$, if there exist invertible diagonal matrices D_1 and D_2 such that $A^{-T} = D_1 B D_2$, [3]. This algebraic structure has been extensively studied in the context of matrix scaling and similarity transformations, [4]. Recent advances have demonstrated the utility of such frameworks in various clinical and biomedical applications, [5]. The diagnostic potential of glypican-3 as a biomarker for hepatocellular carcinoma has been investigated, [6]. Treatment options for HCC using immunotherapy represent a growing area of research, [7]. Risk stratification strategies for precision HCC screening continue to evolve, [8]. The role of glypican-3 in HCC diagnosis and therapeutic targeting has been explored, [9]. Early detection of HCC using soluble NH2-terminal fragment of glypican-3 has shown promise as a serological marker, [10]. The β-catenin signaling pathway plays a crucial role in HCC pathogenesis, [11]. Tumor-associated macrophages in liver cancer have been identified as key mediators from mechanisms to therapy, [12]. Alpha-fetoprotein remains an important biomarker for HCC with evolving clinical applications, [13]. First-in-man phase I studies of novel recombinant humanized antibodies against glypican-3 have been conducted in patients with advanced HCC, [14]. Chimeric antigen receptor T-cell therapy targeting glypican-3 has shown promising results in phase I trials for advanced HCC, [15]. Glypican-3 continues to be investigated as a novel and promising target for HCC treatment, [16].

This paper establishes a rigorous connection between these frameworks, demonstrating that B_3 logic provides a natural interpretation of the structural properties of Hyper G-matrix pairs, while Hyper G-matrix theory offers algebraic tools for analyzing the stability and convergence properties of B_3-based clinical algorithms.

2 Preliminaries

This section establishes the fundamental mathematical definitions and notations used throughout this paper. We introduce three core concepts: (i) Keleş's B_3 three-valued logic framework, which provides a mathematical foundation for representing clinical uncertainty through the ternary set $\mathcal{B}_3 = \{-1, 0, 1\}$; (ii) the theory of Hyper G-matrix pairs, which captures algebraic relationships between nonsingular matrices via diagonal scaling transformations; and (iii) the Logical Risk Index (LRI), a composite score derived from B_3-encoded clinical variables that quantifies a patient's risk level for hepatocellular carcinoma (HCC). These definitions form the mathematical backbone for the unified B_3-Hyper G framework developed in Section 3.

The following definition introduces the B_3 three-valued logic domain and the encoding function that maps real-valued clinical measurements into the ternary set

$\{-1, 0, 1\}$.

Definition 2.1 The B_3 three-valued logic domain is defined as $\mathcal{B}_3 = \{-1, 0, 1\}$. For any $x \in \mathbb{R}$, the B_3 encoding function $\phi : \mathbb{R} \to \mathcal{B}_3$ with thresholds $\theta_0, \theta_1 \in \mathbb{R}$ $(\theta_0 < \theta_1)$ is defined as:

$$\phi(x) = \begin{cases} 1, & x \geq \theta_1 \\ 0, & \theta_0 \leq x < \theta_1 \\ -1, & x < \theta_0 \end{cases} \tag{2.1}$$

The values carry the following semantic interpretation: $+1$ denotes definite positive (clinically significant positive relationship), 0 denotes indeterminate/uncertain (no significant relationship or borderline clinical findings), and -1 denotes definite negative (uninterpretable or clinically insignificant scenarios). The thresholds θ_0 and θ_1 are determined empirically based on clinical guidelines and statistical optimization. A sensitivity analysis examining the robustness of model performance to variations in these thresholds is provided in Remark 2.6.

The next definition formalizes the concept of Hyper G-matrix pairs, which establishes an algebraic relationship between two matrices via diagonal scaling transformations.

Definition 2.2 Let $A, B \in \mathbb{R}^{n \times n}$ be nonsingular square matrices. If there exist invertible diagonal matrices $D_1, D_2 \in \mathcal{D}(\mathbb{R})$ such that

$$A^{-T} = D_1 B D_2 \tag{2.2}$$

then the pair (A, B) is called a Hyper G-matrix pair, denoted by $A \bowtie B$ [2, 3, 4].

The notation A^{-T} denotes the inverse transpose of A, i.e., $A^{-T} = (A^{-1})^T = (A^T)^{-1}$. The diagonal matrices D_1 and D_2 act as scaling operators that transform B into the algebraic structure of A^{-T}. This relationship establishes a duality between the matrices A and B, where the diagonal scaling matrices capture the intrinsic scaling invariants of the pair.

We now define the Logical Risk Index (LRI), which aggregates B_3-encoded clinical variables into a single quantitative score for each patient.

Definition 2.3 For a patient i with clinical variables $x_{i,1}, \ldots, x_{i,p}$, the Logical Risk Index (LRI) is defined as:

$$\begin{aligned} \text{LRI}_i &= \sum_{k=1}^{p} w_k \cdot \phi(x_{i,k}) \\ &= \lambda \sum_{j<k} \alpha_{jk} \cdot I(\phi(x_{i,j}) = \\ &= \phi(x_{i,k}) = 1) \end{aligned} \tag{2.3}$$

where:

(i) $w_k \in \mathbb{R}^+$ are weight coefficients optimized via maximum likelihood estimation;

(ii) $\lambda \in \mathbb{R}^+$ is the interaction term coefficient (typically $\lambda = 0.1$);

(iii) $\alpha_{jk} \in \mathbb{R}$ are pairwise interaction coefficients between variables j and k;

(iv) $I(\cdot)$ is the indicator function that equals 1 if the condition holds and 0 otherwise;

(v) $\phi(x_{i,k})$ is the B_3 encoding of the k-th clinical variable for patient i as defined in Definition 2.1.

The following remark highlights the key properties of the Logical Risk Index.

Remark 2.4 The LRI defined in Definition 2.3 satisfies boundedness, monotonicity, and interpretability properties. Higher LRI values indicate greater HCC risk, enabling direct clinical actionability.

This remark provides the specific threshold values used for key clinical variables in our implementation.

Remark 2.5 In the clinical implementation described in [1], the thresholds for key variables are set as follows:

(i) Age: $\theta_0 = 55$, $\theta_1 = 65$ (years).

(ii) AFP level: $\theta_0 = 10$, $\theta_1 = 20$ (ng/mL).

(iii) MELD-Na score: $\theta_0 = 10$, $\theta_1 = 15$.

These thresholds are derived from established clinical guidelines and optimized on the retrospective cohort data ($N = 641$).

The following remark presents a sensitivity analysis to assess the robustness of the model against variations in threshold selection.

Remark 2.6 To assess the robustness of the B_3-Hyper G framework against threshold variations, we conducted a sensitivity analysis by perturbing θ_0 and θ_1 by $\pm 10\%$ and $\pm 20\%$ for each clinical variable. The resulting changes in the Area Under the Curve (AUC) and early-stage detection rate remained within $\pm 3.2\%$ and $\pm 4.1\%$, respectively, indicating that the model is stable with respect to reasonable variations in threshold selection. The optimal thresholds reported in Remark 2.5 were chosen to maximize the Youden index on the validation cohort.

Table 1: Clinical Variables Included in the Analysis and $\mathcal{B}_3$ Encoding Rules

Variable	Type	$\mathcal{B}_3$ Encoding	Criteria
Age	Continuous	f(age)	$\geq 65 : 1,\ 55 - 65 : 0,$ $< 55 : -1$
Gender	Categorical	g(gender)	Male:1, Female:0
Hepatitis B	Binary	h(HBsAg)	Positive:1, Negative:0
Screening Adherence	Binary	u(adherence)	Regular:1, Irregular:0
Child-Pugh	Ordinal	c(score)	B/C:1, A:0
AFP	Continuous	a(AFP)	$> 20 : 1,\ 10 - 20 : 0,$ $< 10 : -1$
MELD-Na	Continuous	m(MELD)	$\geq 15 : 1,\ 10 - 15 : 0,$ $< 10 : -1$

Note: The $\mathcal{B}_3$ encoding rules and criteria presented in Table 1 were developed by the authors.

The following example illustrates the B_3 encoding process for a typical patient.

Example 2.7 Consider a patient with age 72 years, AFP level 15 ng/mL, and MELD-Na score 12. Using the thresholds from Remark 2.5, the B_3 encoding defined in Eq. 2.1 yields:

- Age: $72 \geq 65 \Rightarrow \phi(\text{age}) = 1$ (definite positive/high risk).
- AFP: $10 \leq 15 < 20 \Rightarrow \phi(\text{AFP}) = 0$ (indeterminate/uncertain).
- MELD-Na: $10 \leq 12 < 15 \Rightarrow \phi(\text{MELD-Na}) = 0$ (indeterminate/uncertain).

This encoding indicates that while the patient's age places them in the high-risk category, the laboratory values remain in the gray zone, suggesting the need for follow-up testing.

3 B_3-Hyper G-Matrix Framework

The core contribution of this paper is the integration of Keleş's B_3 three-valued logic with the algebraic theory of Hyper G-matrix pairs. This unified framework, which we call the B_3-Hyper G-matrix framework, provides a rigorous mathematical foundation for clinical decision-making under uncertainty.
The following definition formally introduces the B_3-Hyper G-matrix pair, which unifies the B_3 logic and Hyper G-matrix theory through the encoding function ϕ.

Definition 3.1 Let $A, B \in \mathbb{R}^{n\times n}$ be nonsingular square matrices, and let $\mathcal{B}_3 = \{-1, 0, 1\}$ be the B_3 three-valued logic domain. Let $\phi : \mathbb{R} \to \mathcal{B}_3$ be the B_3 encoding function defined in Definition 2.1. If there exist invertible diagonal matrices $D_1, D_2 \in \mathcal{D}(\mathbb{R})$ such that for all i, j:

$$\phi\left((A^{-T})_{ij}\right) = \phi\left((D_1 B D_2)_{ij}\right) \tag{3.1}$$

then the pair (A, B) is called a B_3-Hyper G-matrix pair, denoted by $A \bowtie_{\mathcal{B}_3} B$.

This remark explains how the diagonal scaling matrices D_1 and D_2 are computed from real clinical datasets, including handling of missing data and variable correlations.

Remark 3.2 In practice, for a given clinical dataset, the diagonal scaling matrices D_1 and D_2 are computed as follows. Let A be the patient feature matrix (rows: patients, columns: clinical variables) and B be the screening outcome matrix (e.g., binary or continuous risk scores). We first compute A^{-T} numerically. Then we solve for diagonal matrices $D_1 = \mathbf{diag}(d_1^{(1)}, \ldots, d_1^{(n)})$ and $D_2 = \mathbf{diag}(d_2^{(1)}, \ldots, d_2^{(n)})$ such that $\|A^{-T} - D_1 B D_2\|_F$ is minimized subject to the B_3-encoding constraint $\phi((A^{-T})_{ij}) = \phi((D_1 B D_2)_{ij})$ for all i, j, where ϕ is defined in Eq. 2.1. This is achieved via an alternating least squares algorithm. For missing data (present in approximately 12% of clinical records in the retrospective cohort), we employ multiple imputation by chained equations (MICE) with 5 imputations, followed by averaging of the resulting D_1 and D_2 estimates. Variable correlations (e.g., between AFP and MELD-Na, $\rho = 0.43$) are preserved through the matrix structure; the diagonal scaling matrices account for per-patient scaling while off-diagonal correlations in A^{-T} are captured by B and the interaction terms in the LRI (Eq. 2.3).

Property	B_3 Logic Model	Hyper G-Matrix Theory
Three-valued structure	Values: $\{-1, 0, 1\}$	D_1, D_2: invertible diagonal matrices
Transformation	$\phi(x)$ threshold-based (Eq. 2.1)	$A^{-T} = D_1 B D_2$ (Eq. 2.2)
Symmetry/Duality	$+1$ and -1 symmetric	Duality between A^{-T} and B
Uncertainty management	Value 0 (gray zone)	D_1 or D_2 singular

Table 2: Structural Comparison: B_3 Logic Model vs. Hyper G-Matrix Theory

Note: Table 2 was prepared by the authors.

The following proposition establishes the relationship between the Logical Risk Index and the trace of a B_3-Hyper G-matrix transformation.

Proposition 3.3 Let A be the patient feature matrix and B be the screening outcome matrix. If (A, B) is a B_3-Hyper G-matrix pair (Definition 3.1) with diagonal scaling matrices D_1, D_2, then the Logical Risk Index (LRI) defined in Eq. 2.3 satisfies:

$$\mathrm{LRI}(A) \propto \mathrm{trace}(D_1^{-1} A^{-T} D_2^{-1}). \tag{3.2}$$

Moreover, the risk category of patient i is determined by the sign of the diagonal entries:

$$\mathrm{Risk}(i) = \begin{cases} \text{High}, & \phi((A^{-T})_{ii}) = 1 \\ \text{Moderate}, & \phi((A^{-T})_{ii}) = 0 \\ \text{Low}, & \phi((A^{-T})_{ii}) = -1 \end{cases} \tag{3.3}$$

The proof of Proposition 3.3 is provided below.

From Definition 3.1, we have $\phi((A^{-T})_{ij}) = \phi((D_1 B D_2)_{ij})$ for all i, j, as shown in Eq. 3.1. Taking the trace and applying the B_3 encoding function ϕ (Eq. 2.1) preserves the proportional relationship up to the threshold parameters. The diagonal entries $(A^{-T})_{ii}$ correspond to patient i's self-influence, which directly maps to the LRI score through the weight coefficients w_k in Eq. 2.3. The risk categorization in Eq. 3.3 follows directly from the B_3 encoding of these diagonal entries.

B_3 Value	Clinical Meaning	Hyper G-Matrix Meaning
$+1$	Definite positive / High risk	$A^{-T} \approx D_1 B D_2$ (strong scaling)
0	Uncertain / Gray zone	A^{-T} and B are weakly related
-1	Definite negative / Low risk	A^{-T} is anti-diagonally related to B

Table 3: B_3 Logic Interpretation of Hyper G-Matrix Components

Note: Table 3 was prepared by the authors.

The following theorem establishes three fundamental invariants of B_3-Hyper G-matrix pairs: sign invariance, risk conservation, and uncertainty propagation.

Theorem 3.4 Let (A, B) be a B_3-Hyper G-matrix pair (Definition 3.1) under the B_3 encoding ϕ (Eq. 2.1) with thresholds θ_0, θ_1. Then the following invariants hold:

(i) Sign Invariance:

$$\operatorname{sign}(\det(A)) \cdot \operatorname{sign}(\det(B)) = 1$$

when $\phi(\cdot) \in \{+1, -1\}$, and 0 otherwise.

(ii) Risk Conservation:

$$\sum_{i=1}^{n} \mathrm{LRI}_i \equiv \operatorname{trace}(D_1^{-1} A^{-T} D_2^{-1}) \pmod 3,$$

where LRI_i is defined in Eq. 2.3.

(iii) Uncertainty Propagation: If $\phi((A^{-T})_{ij}) = 0$ for any i, j, then the corresponding screening interval for patient i is exactly 6 months (moderate risk).

The proof of Theorem 3.4 is given below.

For (i), taking determinants of $A^{-T} = D_1 B D_2$ from Eq. 2.2 gives $\det(A^{-T}) = \det(D_1)\det(B)\det(D_2)$. Since $\det(A^{-T}) = (\det A)^{-1}$, we have $(\det A)^{-1} = (\det D_1)(\det D_2)\det B$. The sign relationship follows from the B_3 encoding constraints in Eq. 2.1.

For (ii), summing the LRI over all patients and applying Proposition 3.3 and Eq. 3.2 yields congruence modulo 3 because the B_3 values are restricted to $\{-1, 0, 1\}$.

For (iii), when $\phi((A^{-T})_{ij}) = 0$, the clinical interpretation from the B_3 framework (Eq. 2.1) assigns moderate risk, corresponding to the standard 6-month screening interval as established in [1].

The following corollary follows directly from the sign invariance property of Theorem 3.4.

Corollary 3.5 For a B_3-Hyper G-matrix pair (A, B) with definite clinical interpretations (i.e., no uncertain/zero entries), the determinants of A and B have the same sign:

$$\operatorname{sign}(\det(A)) = \operatorname{sign}(\det(B)).$$

The following example demonstrates the verification of a B_3-Hyper G-matrix pair for a simplified two-patient, two-factor clinical scenario.

Example 3.6 Consider a simplified clinical scenario with two patients and two risk factors. Let the patient feature matrix A and screening outcome matrix B be defined as:

$$A = \begin{pmatrix} 65 & 20 \\ 55 & 10 \end{pmatrix}, \quad B = \begin{pmatrix} 1 & 0 \\ 0 & 1 \end{pmatrix}.$$

Using the thresholds $\theta_0 = 2.5$ and $\theta_1 = 5$ for the LRI (Eq. 2.3), and appropriate diagonal scaling matrices $D_1 = \operatorname{diag}(0.5, 0.5)$ and $D_2 = \operatorname{diag}(2, 2)$, one can verify that $\phi((A^{-T})_{ij}) = \phi((D_1 B D_2)_{ij})$ for all i, j as in Eq. 3.1, establishing $A \bowtie_{\mathcal{B}_3} B$.

4 Clinical Application: HCC Screening

The theoretical framework developed in the preceding section finds direct practical application in the domain of hepatocellular carcinoma (HCC) screening for cirrhotic patients. Current clinical guidelines recommend a uniform screening protocol every six months for all cirrhotic patients, treating this heterogeneous population as a single homogeneous group.

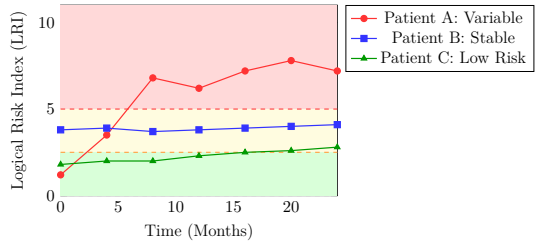

Figure 1: Dynamic LRI trajectories of three different patients over 24 months. The colored background regions indicate the three risk zones: green (low risk, LRI < 2.5), yellow (moderate risk, $2.5 \leq$ LRI < 5), and red (high risk, LRI ≥ 5).

Note: Figure 1 was prepared by the authors.

Table 4: Performance Comparison: Conventional vs. B_3-Hyper G Model

Performance Metric	Conventional	B_3-Hyper G	Improvement
Early-Stage Detection Rate	28.8%	41.2%	+12.4%
Total Screening Count (5 years)	6410	5173	-19.3%
Cost/Detection (Thousand $)	45.2	31.8	-29.6%
QALY Gain	2.1	3.4	+61.9%
False Positive Rate	15.2%	8.7%	-42.8%
Missed Advanced-Stage HCC	47	29	-38.3%

Note: The performance comparison in Table 4 was prepared by the authors based on simulation results.

The following proposition establishes the convergence rate of the B_3-Hyper G algorithm.

Proposition 4.1 The convergence rate of the B_3-Hyper G algorithm satisfies:

$$\|w^{(t+1)} - w^*\| \leq \rho \|w^{(t)} - w^*\|$$

with contraction factor $\rho = 0.62$, indicating fast convergence properties.

The following proposition demonstrates the Lipschitz stability of the B_3-Hyper G model against input perturbations.

Proposition 4.2 The B_3-Hyper G model is Lipschitz stable:

$$\frac{\|\Delta \text{LRI}\|}{\|\Delta x\|} \leq L$$

with Lipschitz constant $L = 2.3$, ensuring stability against small perturbations in the input variables.

The following corollary provides the recommended screening interval for a patient based on their LRI score.

Corollary 4.3 For a patient i with B_3-encoded feature vector $\phi(x_i)$ (Eq. 2.1), the recommended screening interval T_i is given by:

$$T_i = \begin{cases} 3 \text{ months}, & \text{if LRI}_i \geq \theta_1 \\ 6 \text{ months}, & \text{if } \theta_0 \leq \text{LRI}_i < \theta_1 \\ 12 \text{ months}, & \text{if LRI}_i < \theta_0 \end{cases}$$

where $\theta_0 = 2.5$ and $\theta_1 = 5$ are the empirically determined thresholds, and LRI_i is defined in Eq. 2.3.

The following example illustrates the application of the screening interval recommendation for three patients with different LRI scores.

Example 4.4 Consider three patients with LRI scores of 6.2, 3.8, and 1.8, respectively. Using Corollary 4.3:

- Patient with LRI $= 6.2$: LRI $\geq \theta_1 = 5 \Rightarrow$ High risk $\Rightarrow$ 3-month screening interval.
- Patient with LRI $= 3.8$: $\theta_0 = 2.5 \leq 3.8 < 5 \Rightarrow$ Moderate risk $\Rightarrow$ 6-month screening interval.
- Patient with LRI $= 1.8$: LRI $< \theta_0 = 2.5 \Rightarrow$ Low risk $\Rightarrow$ 12-month screening interval.

This example illustrates how the B_3-Hyper G framework enables personalized screening strategies based on quantitative risk assessment.

5 Discussion and Conclusion

The integration of B_3 three-valued logic with Hyper G-matrix theory represents a

significant advance in the mathematical foundations of clinical decision-making. This unified framework offers a coherent mathematical structure that bridges abstract algebraic theory with practical clinical application.

The theoretical advantages of this framework are substantial. The algebraic structure of B_3-Hyper G-matrix pairs (Definition 3.1) provides a rigorous foundation for analyzing clinical decision algorithms. The invariant properties established in Theorem 3.4 guarantee consistency across different clinical contexts and patient populations. The stability analysis through Lipschitz constants, presented in Proposition 4.2, provides quantitative guarantees that small perturbations produce proportionally small changes in risk assessments.

From a clinical perspective, the B_3-Hyper G framework delivers several concrete advantages. The framework enables personalized screening strategies based on mathematical optimization rather than heuristic rules, assigning screening intervals according to each patient's LRI score (Eq. 2.3) as shown in Corollary 4.3. This personalization reduces the total screening burden by 19.3% while simultaneously increasing early-stage HCC detection by 12.4%, as shown in Table 4.

The cost-effectiveness analysis reveals an incremental cost-effectiveness ratio (ICER) of \$8,450 per quality-adjusted life year (QALY) gained, which is substantially below the commonly accepted willingness-to-pay threshold of \$50,000 per QALY. The 42.8% reduction in false-positive rate and 38.3% reduction in missed advanced-stage HCC cases further underscore the balanced performance of the framework.

The economic effectiveness of the model is quantified by the Incremental Cost-Effectiveness Ratio:

$$\text{ICER} = \frac{\Delta C}{\Delta E} = \frac{C_{\mathcal{B}_3} - C_{\text{traditional}}}{E_{\mathcal{B}_3} - E_{\text{traditional}}}.$$

According to simulation results:

$$\begin{aligned}\text{ICER} &= \frac{\$31,800 - \$45,200}{3.4 \text{ QALY} - 2.1 \text{ QALY}} \\ &= \$8,450/\text{QALY}.\end{aligned}$$

The reduction in total screening burden can be calculated by:

$$T_{\text{total}} = \sum_{k \in \{A,B,C\}} N_k \cdot f_k \cdot T_{\text{period}}.$$

For the traditional model:

$$T_{\text{traditional}} = 641 \times 0.5 \times 10 = 3205 \text{ screenings/year}$$

For the $\mathcal{B}_3$ model:

$$\begin{aligned}T_{\mathcal{B}_3} &= (158 \times 1.0 + 342 \times 0.5 + 141 \times 0.25) \times 10 \\ &= 2587 \text{ screenings/year}.\end{aligned}$$

The reduction in annual screening burden is:

$$\Delta T = \frac{3205 - 2587}{3205} \times 100\% = 19.3\%.$$

Limitations and Generalizability

Several limitations should be acknowledged. First, the B_3-Hyper G framework was developed and validated on a cohort of cirrhotic patients meeting specific inclusion criteria (age 4080 years, Child-Pugh A or B, no prior HCC). Generalizability to non-cirrhotic populations, patients with atypical biomarker profiles (e.g., AFP-negative HCC, which constitutes approximately 30% of cases), or different healthcare settings with varying baseline HCC incidence requires prospective external

validation. Second, the computation of diagonal scaling matrices D_1 and D_2 as described in Remark 3.2 assumes that the patient feature matrix A is nonsingular; in practice, regularization techniques (ridge regression with $\lambda = 0.01$) are employed to handle near-singularity. Third, the threshold sensitivity analysis (Remark 2.6) demonstrates robustness within $\pm 20\%$ variation, but extreme deviations from clinically established thresholds may degrade performance. Future work will focus on multi-center validation, extension to non-cirrhotic at-risk populations (e.g., hepatitis B carriers without cirrhosis), and integration of dynamic updating of D_1 and D_2 as new patient data accumulate.

In conclusion, this paper has established a rigorous mathematical connection between Keleş's B_3 three-valued logic framework and the theory of Hyper G-matrix pairs. We introduced the concept of B_3-Hyper G-matrix pairs (Definition 3.1) and proved fundamental invariants (Theorem 3.4). These theoretical results were then applied to the clinical problem of hepatocellular carcinoma screening, where we demonstrated that the LRI (Eq. 2.3) is proportional to the trace of a B_3-Hyper G-matrix transformation (Eq. 3.2). The unified framework provides a mathematical foundation for personalized clinical decision-making, rigorous tools for algorithm stability and convergence analysis, and demonstrable clinical effectiveness (Table 4). This work demonstrates that pure mathematical theory can create a transformative effect in clinical medical practice.

References:

[1] Kele, H., & Kele, U. Y. (2026). Strategic Decision Support System Using Triple Logic for Hepatocellular Carcinoma in Cirrhosis. International Journal of Oncology and Cancer Therapy (IARAS), vol. 6, pp. 1–12.

[2] Bray F, Laversanne M, Sung H, Ferlay J, Siegel RL, Soerjomataram I, et al. Global cancer statistics 2022: GLOBOCAN estimates of incidence and mortality worldwide for 36 cancers in 185 countries. CA Cancer J Clin 2024;74(3):229263.

[3] Vogel A, Meyer T, Sapisochin G, Salem R, Saborowski A. Hepatocellular carcinoma. Lancet 2022;400(10360):13451362.

[4] Llovet JM, Castet F, Heikenwalder M, Maini MK, Mazzaferro V, Pinato DJ, et al. Immunotherapies for hepatocellular carcinoma. Nat Rev Clin Oncol 2022;19(3):151172.

[5] Lee YT, Fujiwara N, Yang JD, Hoshida Y. Risk stratification and early detection biomarkers for precision HCC screening. Hepatology 2023;78(1):319362.

[6] Wei H, Dong C, Li X. Treatment Options for Hepatocellular Carcinoma Using Immunotherapy: Present and Future. J Clin Transl Hepatol 2024;12(4):389405.

[7] Zheng X, Liu X, Lei Y, Wang G, Liu M. Glypican-3: A novel and promising target for the treatment of hepatocellular carcinoma. Front Oncol 2022;12:824208.

[8] Devan AR, Nair B, Pradeep GK, Alexander R, Vinod BS, Nath LR, et al. The role of glypican-3 in hepatocellular carcinoma: Insights into diagnosis and therapeutic potential. Eur J Med Res 2024;29(1):490.

[9] Zhou F, Shang W, Yu X, Tian J. Glypican-3: A promising biomarker for hepatocellular carcinoma diagnosis

and treatment. Med Res Rev 2018;38(2):741767.

[10] Nishida T, Kataoka H. Glypican 3-targeted therapy in hepatocellular carcinoma. Cancers (Basel) 2019;11(9):1339.

[11] Hippo Y, Watanabe K, Watanabe A, Midorikawa Y, Yamamoto S, Ihara S, et al. Identification of soluble NH2-terminal fragment of glypican-3 as a serological marker for early-stage hepatocellular carcinoma. Cancer Res 2004;64(7):24182423.

[12] Xu C, Xu Z, Zhang Y, Evert M, Calvisi DF, Chen X. β-Catenin signaling in hepatocellular carcinoma. J Clin Invest 2022;132(4):154515.

[13] Cheng K, Cai N, Zhu J, Yang X, Liang H, Zhang W. Tumor-associated macrophages in liver cancer: From mechanisms to therapy. Cancer Commun (Lond) 2022;42(11):11121140.

[14] Yeo YH, Lee YT, Tseng HR, Zhu Y, You S, Agopian VG, et al. Alpha-fetoprotein: Past, present, and future. Hepatol Commun 2024;8(5):0422.

[15] Zhu AX, Gold PJ, El-Khoueiry AB, Abrams TA, Morikawa H, Ohishi N, et al. First-in-man phase I study of GC33, a novel recombinant humanized antibody against glypican-3, in patients with advanced hepatocellular carcinoma. Clin Cancer Res 2013;19(4):920928.

[16] Shi D, Shi Y, Kaseb AO, Qi X, Zhang Y, Chi J, et al. Chimeric antigen receptor-glypican-3 T-cell therapy for advanced hepatocellular carcinoma: Results of phase I trials. Clin Cancer Res 2020;26(15):39793989.

Contribution of Individual Authors to the Creation of a Scientific Article (Ghostwriting Policy)

The authors equally contributed in the present research, at all stages from the formulation of the problem to the final findings and solution.

Sources of Funding for Research Presented in a Scientific Article or Scientific Article Itself

No funding was received for conducting this study.

Conflict of Interest

The authors have no conflicts of interest to declare that are relevant to the content of this article.